

Accounts

Helical Supramolecular Architectures of Self-Assembled Linear π-Systems

Vakayil K. Praveen, Sukumaran S. Babu, Chakkooth Vijayakumar, Reji Varghese, and Ayyappanpillai Ajayaghosh*

Photosciences and Photonics Group, Chemical Sciences and Technology Division, National Institute for Interdisciplinary Science and Technology (NIIST), CSIR, Trivandrum 695 019, India

Received May 7, 2008; E-mail: ajayaghosh62@gmail.com

The present account describes the summary of the recent developments to the design of helical self-assemblies of linear π-conjugated molecules, particularly of oligo(*p*-phenylenevinylenes) (OPVs) and oligo(*p*-phenyleneethynylenes) (OPEs). The design strategy involves functionalization of π-conjugated backbones with achiral and chiral alkoxy side chains and hydroxymethyl end groups. Self-organization of these molecules in nonpolar hydrocarbon solvents resulted in a variety of supramolecular architectures such as tapes, helices, vesicles, and tubules. These supramolecular structures eventually lead to the formation of entangled networks resulting in gelation of solvents. It has been observed that OPVs in nonpolar solvents prefer to form supramolecular tapes whereas the corresponding OPEs form nano- to microsized vesicles and bundled fibers. Attachment of chiral motifs to OPVs and OPEs resulted in the formation of helical structures with a preferred handedness. The "sergeants and soldiers" co-assembly approach to chirality induction and amplification is efficient in these systems in the gel state. These results highlight the importance of the subtle difference in the strength of π–π interaction in gel forming linear π-systems to the creation of hierarchical architectures with different size and shape, particularly helical structures.

1. Introduction

Nature has the unique ability to create nano- to microsized helical architectures as in the cases of DNA, collagen, proteins, and virus. These structures are stabilized through weak noncovalent interactions and are responsible for their specific biological functions. The helical bias in such systems is created due to the presence of asymmetric carbon atoms present in the molecular building blocks. Chemist's passion towards natural helical structures has lead to the creation of a variety of artificial helical assemblies of synthetic molecules using the principles of supramolecular chemistry.[1–6] This interesting research programme not only helped to unravel the intricacies of Nature's helical programming technique, but also led to the construction of a variety of artificial helical architectures with promising application in the areas of chirotechnology and supramolecular electronics.[5–7] The properties of these artificial helical assemblies are found to be as fascinating as their natural counterparts which have been the major source of inspiration for scientists to focus their attention into this active area of research.

Among different class of molecules, helical architectures created from linear π-systems are of special interest due to their potential applications as active components in organic electronic devices.[7,8] Linear π-systems based on phenylenevinylenes, phenyleneethynylenes, phenylenes, and thiophenediyls have been extensively utilized for this purpose due their ability to form stable self-assemblies. Presence of a chiral handle on a π-conjugated system is capable of biasing the overall packing of the molecules in a hierarchical self-assembly. Upon self-assembly, the peripheral chiral centers present in the side chains or as end functional groups will express the chirality at the supramolecular level with amplification. Such amplification is governed by the intrinsic conformational chirality of the self-assembly which is an outcome of careful matching of noncovalent interactions present.[1–5] The strategies which are commonly used to induce supramolecular chirality in the co-assembly of achiral and chiral molecules are based on the "sergeants and soldiers principle" and the "majority rules."[3c,4] These concepts were introduced for the preparation of helical polyisocyanates by Green and co-workers which were later extended to dynamic supramolecular assemblies.[4a,4b] These rules illustrate that, co-assembly of achiral molecules (soldiers) with a small amount of chiral molecules (sergeants) may bias the overall organization of the molecular assemblies towards the chiral sense of the latter resulting in helical supramolecular structures with a preferred handedness (either P or M) or have a slight majority of one particular chiral sense over other (majority rule). These chiral induction processes could be monitored via circular dichroism (CD) spectroscopy[9] and high-resolution microscopic techniques such as scanning elec-

Published on the web October 10, 2008; doi:10.1246/bcsj.81.1196

tron microscopy (SEM), atomic force microscopy (AFM), scanning tunnelling microscopy (STM), and transmission electron microscopy (TEM).

2. Supramolecular Helical Structures of Electronically Active Molecules

Meijer, Schenning, and co-workers have made significant contributions to the design of self-assembled helical structures of OPVs and oligo(thiophene)s (OTs). For example, OPVs functionalized with chiral alkyl side chains and ureido-*s*-triazine quadruple H-bonding units (OPVUTs) self-assemble to form left-handed helical columns as evidenced from the bisignate circular dichroism (CD) signal (Figure 1).[10] Detailed temperature and concentration dependent optical and chiroptical studies have shown that the stability of these self-assembled stacks increases with conjugation length due to the favorable π–π interactions.[10b] Detailed spectroscopic analysis of the properties of the aggregates suggests a nucleation–growth pathway which is characterized by a size-dependent association constant and a remarkable degree of cooperativity (Figure 2).[10c] The initial step of this process is the formation of dimers from monomers as a result of strong quadruple H-bonding. Upon cooling the dimers will be converted into first disordered stacks and then pre-aggregates. In the pre-aggregates the molecules are positionally locked due to cooperativity of several noncovalent interactions present. In the next step, pre-aggregates undergo a coil–helix transition to form a chiral nucleus which triggers the elongation–growth pathway. Finally, the clustering of self-assemblies occurs once they attained the cooperative stack length.

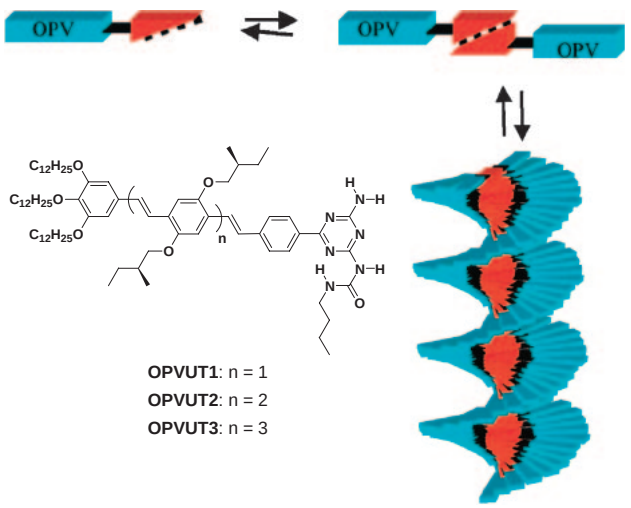

Figure 1. Schematic representation of the hierarchical helical organization of OPVUTs. Reprinted from Ref. 10a with permission. Copyright 2001 American Chemical Society.

Chiral OPVs upon functionalization with diamino triazine moieties (OPVT**1** and OPVT**2**, Chart 1) self-assemble to hexameric π-conjugated rosette structures and subsequently grow into chiral tubular objects.[11] STM images showed chiral hexameric rosette structures lying flat on the surface with the diamino triazine moieties forming a hydrogen-bonded cavity. AFM and CD studies have shown that in nonpolar solvents these rosette structures stack on each other through π–π interactions to form tubular self assemblies.

Recently, it has been demonstrated that functionalization of OPVs with nucleotides (OPVNT) allows the complementary interaction of single-stranded oligodeoxyadenylic acid (ODA) in aqueous solutions resulting in right-handed helical structures (Chart 2a).[12a] Through another approach, chiral organisations of OPVs (OPVT**3**) were achieved using single-strand DNA (ssDNA) as the template resulting in the formation of new functional hybrid materials (Chart 2b).[12b] Chirality of the templated DNA was expressed through the right-handed

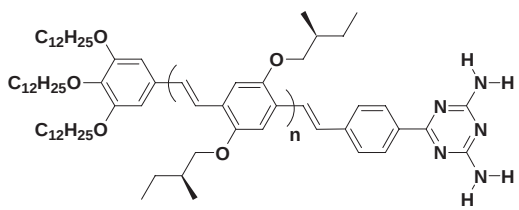

OPVT1: n = 1

OPVT2: n = 2

Chart 1.

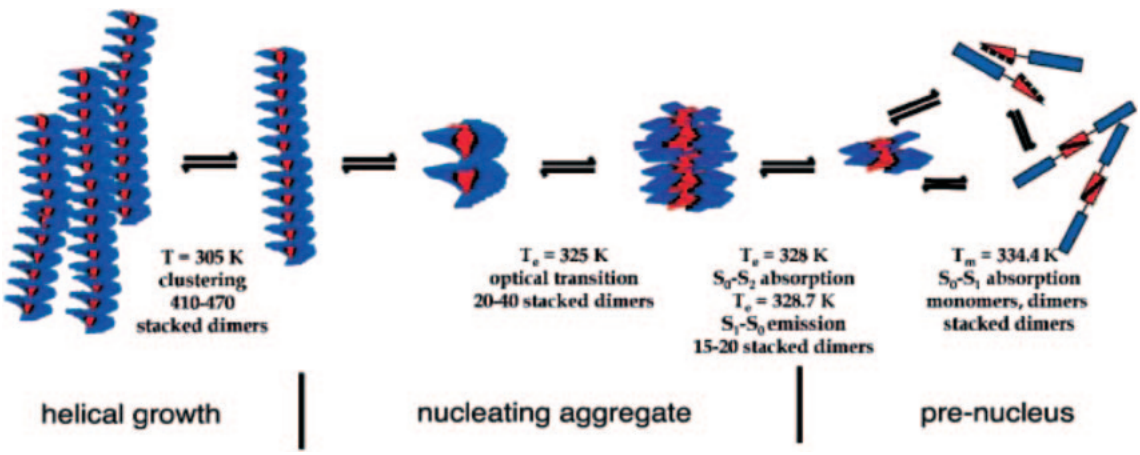

Figure 2. Schematic representation of the hierarchical self-assembly of OPVUT2 in solution. The proposed scheme is based on the temperature and concentration dependent optical and chiroptical studies. Reprinted from Ref. 10c with permission. Copyright 2006 American Association for the Advancement of Science.

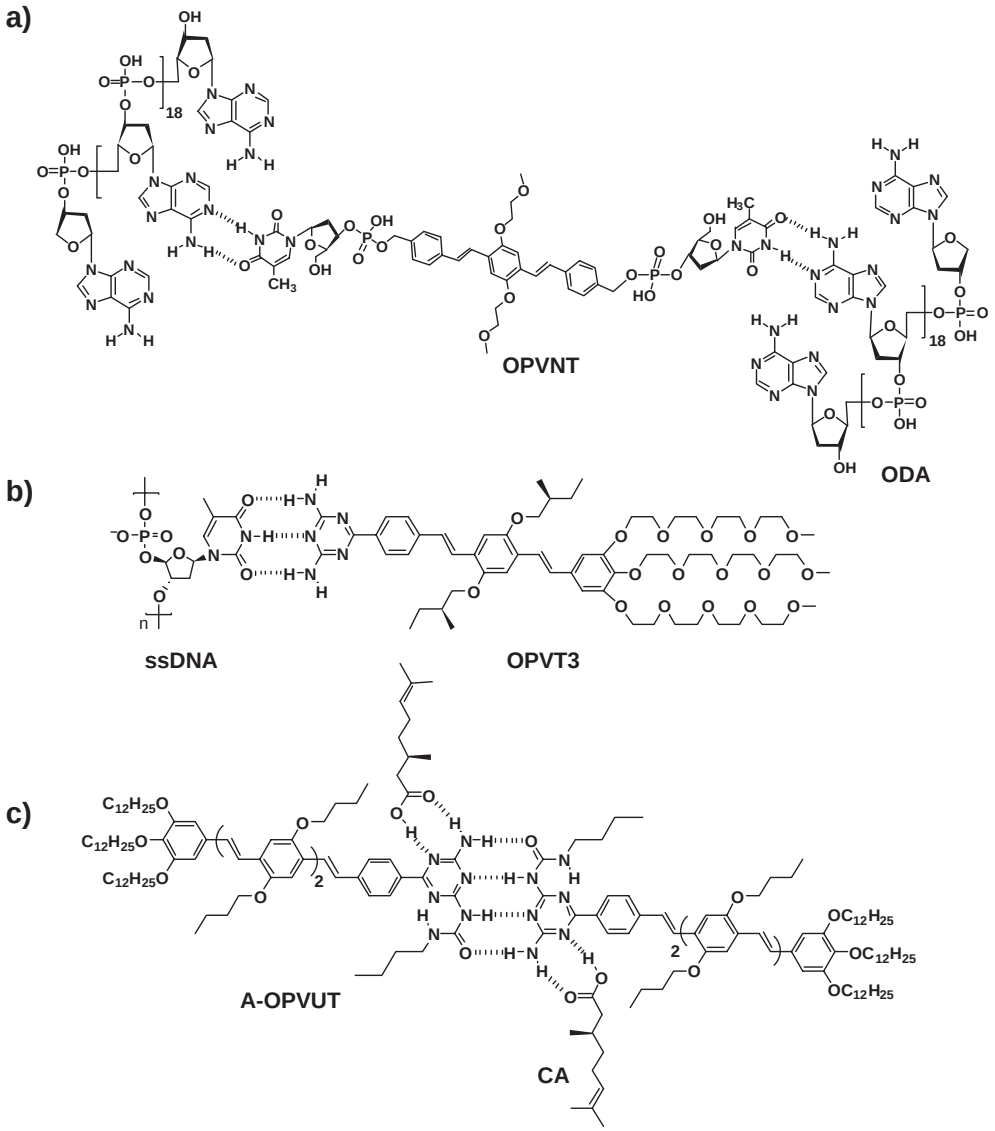

Chart 2.

helical arrangement of the OPV units. Recently, Meijer, Schenning, and co-workers have demonstrated an elegant method to induce chirality in supramolecular assemblies by exploiting host–guest interaction between chiral acids and hydrogen-bonded assembly of achiral OPVs (Chart 2c).[12c] Complexation of chiral citronellic acid (CA) with hydrogen-bonded dimers of A-OPVUT resulted in chirality induction and amplifications through the nucleation–growth mechanism. Detailed understanding of these chiroptical processes led to the mechanistic pathways of chiral induction.

Introduction of amphiphilicity into a π-conjugated backbone facilitates the formation of diverse aggregate morphology depending upon the molecular shape, hydrophobic/hydrophilic balance and solution condition.[8,13] In the case of amphiphilic π-conjugated molecules, the main driving force behind the self assembly is the hydrophobic π-stacking interactions as illustrated with OPVA**1**–A**3** (Chart 3) having varying hydrophobic/hydrophilic balance.[14] Detailed dynamic light scattering (DLS) and scanning confocal microscopy studies showed that the dumbbell-shaped OPVA**2** and OPVA**3** self-assemble to form vesicular aggregates. Absorption and CD studies of these assemblies in aqueous solution revealed the formation of chiral H-type aggregates through the 1-D stacking of OPV units.[14b]

Amphiphilic sexithiophenes substituted with chiral and achiral penta(ethyleneoxide) chains, OTA**1** and OTA**2**, respectively self-assemble to form helical structures (Figure 3).[15] Detailed UV–vis absorption, fluorescence, circular dichroism, and circularly polarized luminescence studies revealed that these compounds form chiral aggregates in polar solvents and in the solid state. AFM analysis of OTA**1** on silicon wafer indicates the formation of nanoropes with left-handed supramolecular helicity which was not observed in the self-assembly of the achiral analogue OTA**2**.

Shinkai and co-workers have demonstrated the formation of one-dimensional left-handed helical structures from the self-assembly of cholesterol-appended quater-, quinque-, and sexithiophene derivatives (Figure 4a).[16] The helical organization of these systems is influenced by strong π-stacking between the π-blocks and van der Waals forces between the

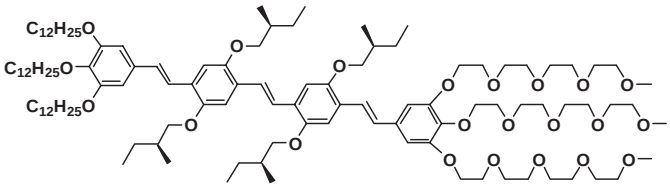

OPVA1

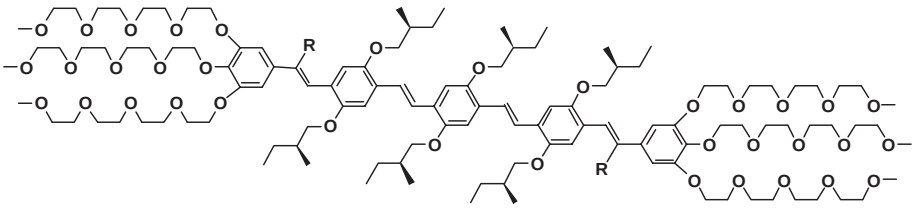

OPVA2: R = H

OPVA3: R = CN

Chart 3.

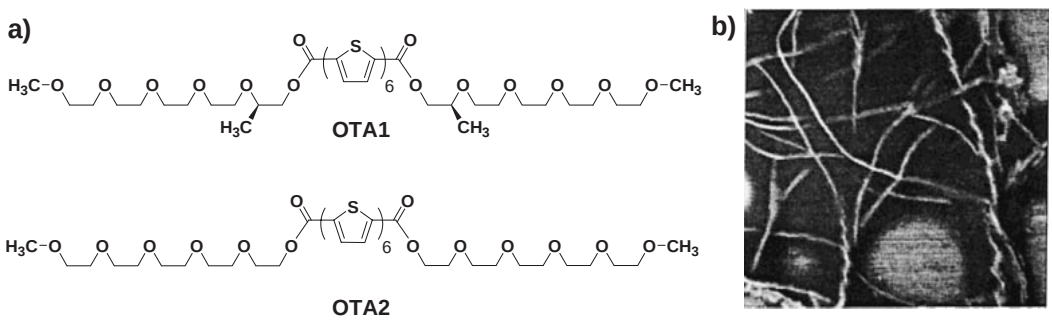

Figure 3. (a) Molecular structure of amphiphilic sexithiophenes. (b) Tapping-mode AFM phase image of OTA**1** on silicon wafer, showing left-handed helical aggregates. Reprinted from Ref. 15b with permission. Copyright 2002 American Chemical Society.

cholesteryl groups. These interactions are further reinforced by strong directional amide H-bonding. The formation of left-handed helical structures was confirmed by detailed optical, chiroptical, and morphological studies. For example, CD studies showed a negative Cotton effect in the π–π^* transition region of thiophene chromophores which indicates that the chromophores are organized in a helical sense with their dipoles oriented in an anticlockwise direction. Furthermore, AFM analysis revealed information regarding the formation of one-dimensional left-handed helical assemblies (Figures 4b–4d).

Lee and co-workers have extensively studied the supramolecular assembly of oligo(*p*-phenylene) amphiphilic molecules (OPAs) which are functionalized with different self-assembling motifs.[3d,13b,13c] A dumbbell-shaped molecule OPA**1** (Figure 5) in aqueous solution self-assembles to form cylindrical micelles in which the molecules are aligned perpendicular to the cylindrical axis.[17a] However, the rod segments stack on top of each other with mutual rotation in the same direction to avoid steric hindrance between the bulky dendritic wedges. Consequently, the stacking of the aromatic rod segments leads to helical objects consisting of hydrophobic aromatic cores surrounded by hydrophilic dendritic segments that are exposed to the aqueous environment, as evident from the CD and TEM studies (Figure 5). The observed supramolecular handedness is believed to arise from steric constraints imposed by the chiral centers in the dendritic wedges.

The dumbbell-shaped molecule OPA**2** (Chart 4) consisting of a hexa *para*-phenylene rod and aliphatic polyether dendrons based on a tetrahedral core, which are covalently linked at both ends of the rod segment, self-assembles into well-defined left-handed helical cylinders.[17b] The diameter of these cylinders matches approximately with the length of one molecule as evident from the TEM analysis. These helical structures transform into capsule-like structures upon the addition of guest molecule such as 4-bromonitrobenzene. This reversible transformation between helical strands and nanocages in response to the addition of guest molecules is attributed to the intercalation of aromatic substrates within the rod segments. As a result, the packing of the rod segments changes from a twisted to a parallel arrangement. Such a packing will allow more space for the guest molecules.

3. π-Conjugated Organogels Derived from Self-Assembled Oligo(*p*-phenylenevinylene)s

Among the various classes of π-conjugated systems, oligo-

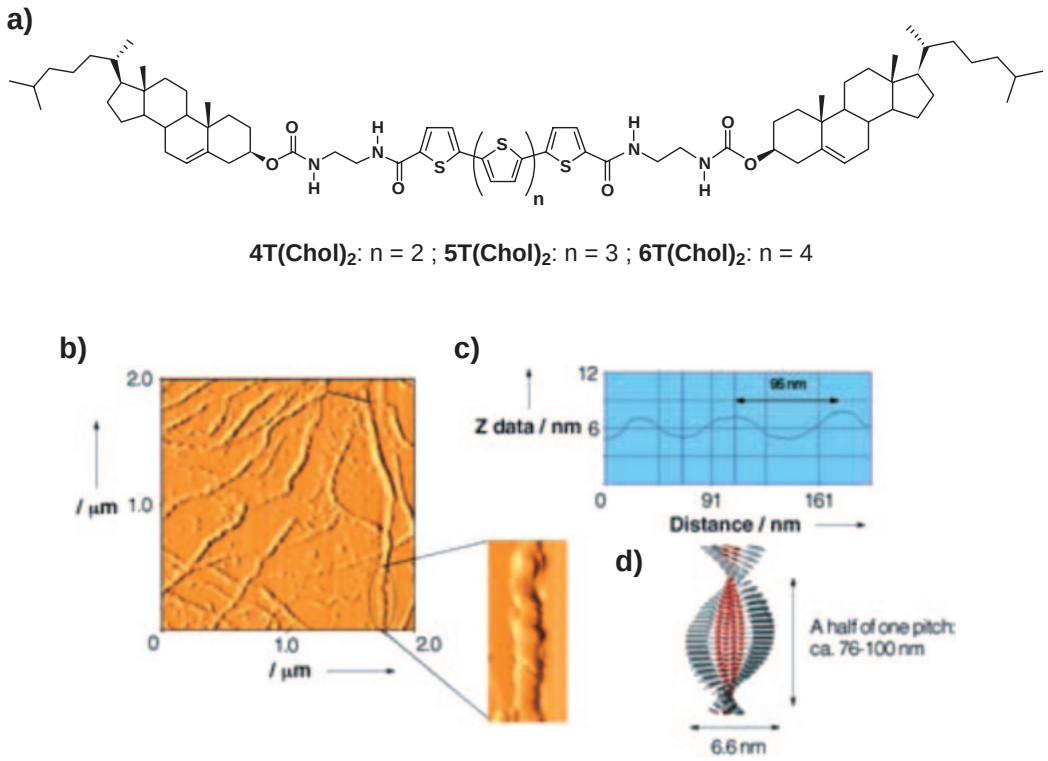

Figure 4. (a) Molecular structure of cholesterol appended thiophene derivatives. (b) AFM image of 4T-$(Chol)_2$, (c) the height profile along the solid line in Figure 4b, and (d) schematic illustration of the helical fiber of 4T-$(Chol)_2$. Reprinted from Ref. 16 with permission. Copyright 2005 Wiley-VCH.

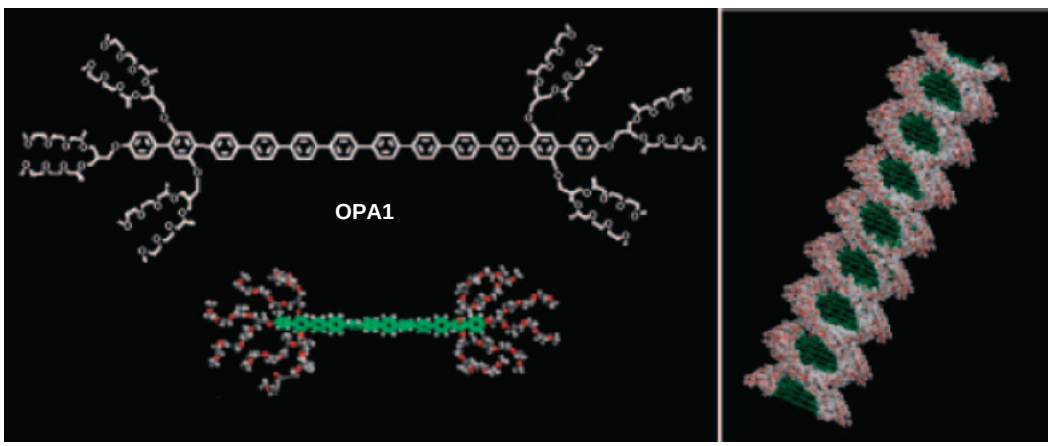

Figure 5. Molecular structure of OPA**1** and representation of a helical nanofiber. Reprinted from Ref. 17a with permission. Copyright 2005 American Chemical Society.

(*p*-phenylenevinylene)s (OPVs) has received considerable attention because of their unique opto-electronic properties.[18] Recently, several new approaches have been developed to construct well-organized chromophoric assemblies of OPVs.[7b,8] It has been shown that self-assembled OPVs are able to gelate nonpolar hydrocarbon solvents due to the formation of supramolecular architectures of different size and shape (Figure 6a).[12c,19–21] For example, OPV**1** and OPV**2**, functionalized with alkoxy side chains and hydroxymethyl end functional groups form organogels in aliphatic and aromatic nonpolar solvents at very low concentrations (<2 mM) (Figure 6b).[19,20]

Insights about the morphology of the OPV gels were obtained from microscopic techniques such as SEM, AFM, and TEM.[20] SEM images of OPV**1** gel in toluene (Figure 6c) showed intertwined three-dimensional network structures composed of supramolecular tapes of 50–100 nm width and several micrometer lengths. The TEM studies of OPV**1** from a dilute toluene solution provided more information about the morphology of self-assembled textures (Figure 6d). The TEM pictures showed the presence of isolated tapes of 20–200 nm width and several micrometers in length. The alternate dark and bright regions observed are the indication of the twisted morphology of the fibers. The AFM analysis of OPV**1** in dodecane (1×10^{-5} M) revealed the formation of

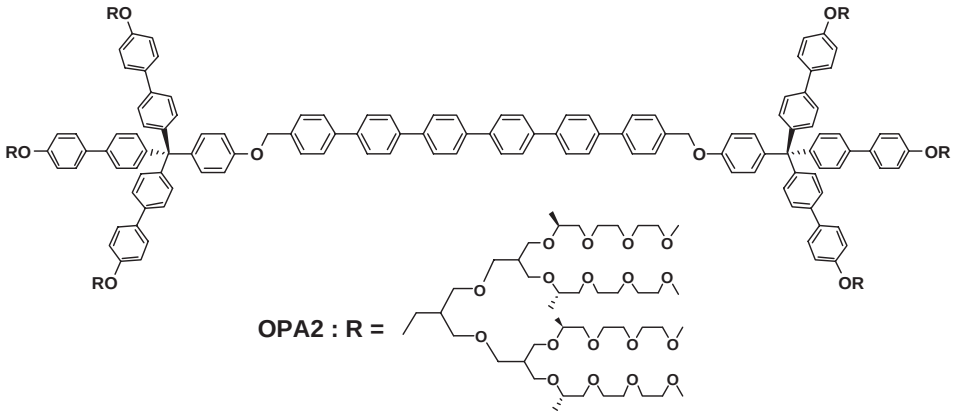

Chart 4.

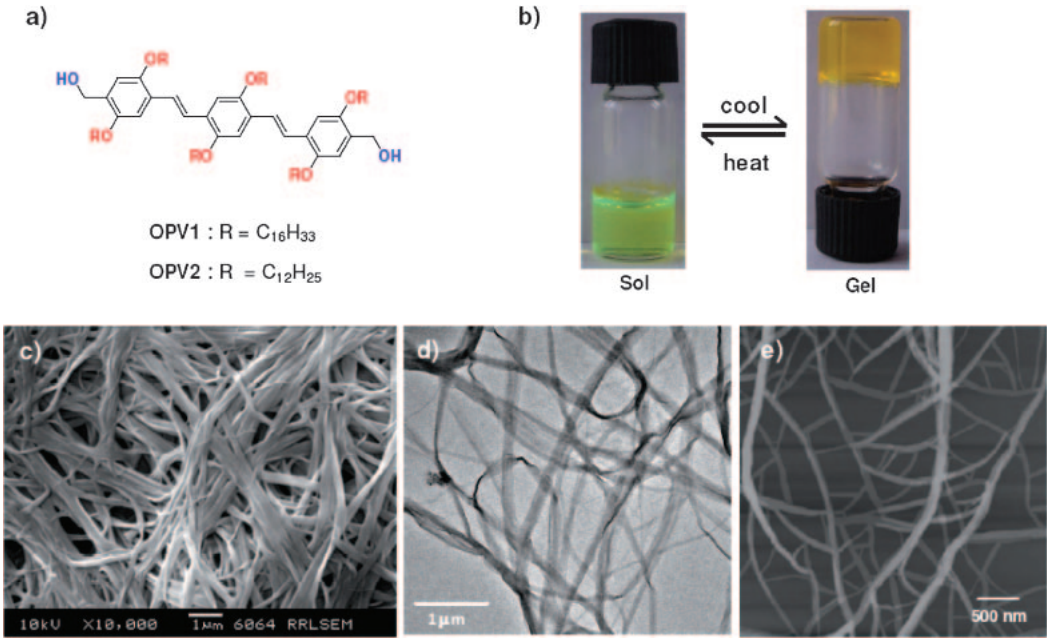

Figure 6. (a) Molecular structure of the gel forming OPVs. (b) Photograph of OPV**1** in cyclohexane before and after gelation (critical gelator concentration, CGC = 1.1 mM). (c) SEM image of toluene gel (2.8 mM), (d) TEM image of a toluene solution (1×10^{-4} M) evaporated on a carbon grid, and (e) AFM tapping mode height image of a dodecane solution (1×10^{-5} M) drop casted on freshly cleaved mica. Reprinted from Ref. 19b with permission. Copyright 2007 American Chemical Society.

supramolecular tapes of 5–15 nm thickness with 35–175 nm width and several micrometers in length (Figure 6e), which is in support to the morphological features observed in SEM and TEM images. X-ray diffraction (XRD) pattern of a xerogel obtained from OPV**1** showed well-resolved diffraction patterns, which indicate the long-range order of molecules within the self-assembly. Based on these results we proposed that the supramolecular tape like morphology of OPV self-assembly is a result of multi layer lamellar assemblies of molecules through hydrogen-bonding, π-stacking, and van der Waals interactions. The extended growth of these assemblies results in twisted tapes to form networks. This facilitates the immobilization of large volumes of solvents within and between the networks, resulting in gelation. Detailed optical and morphological investigations revealed that end functional groups, alkyl chains and solvents have dramatic influence on the gelation and the related properties of these molecules. Recently, it has been shown that the gelation of OPVs facilitate the transfer of excitation energy via resonance energy transfer (RET) exclusively from the self-assembled nanostructures to entrapped acceptor molecules.[19,22]

4. Chirality Transfer via Self-Assembly

Helical structures of chromophores and rigid π-systems can be created through incorporation of chiral side chains followed by self-assembly.[1–5] Presence of the asymmetric carbon induces a bias during the supramolecular organization of the molecules resulting in a preferred handedness. Recently, we have demonstrated that the presence of chiral handles have profound effect in the gelation and the supramolecular chirality as in the case of OPV derivatives bearing chiral (*S*)-3,7-dimethyloctyloxy side chains and hydroxymethyl end groups (Figure 7a).[23] The chiral COPV**1** with six chiral side chains failed to form gels, where as the chiral molecule COPV**2**

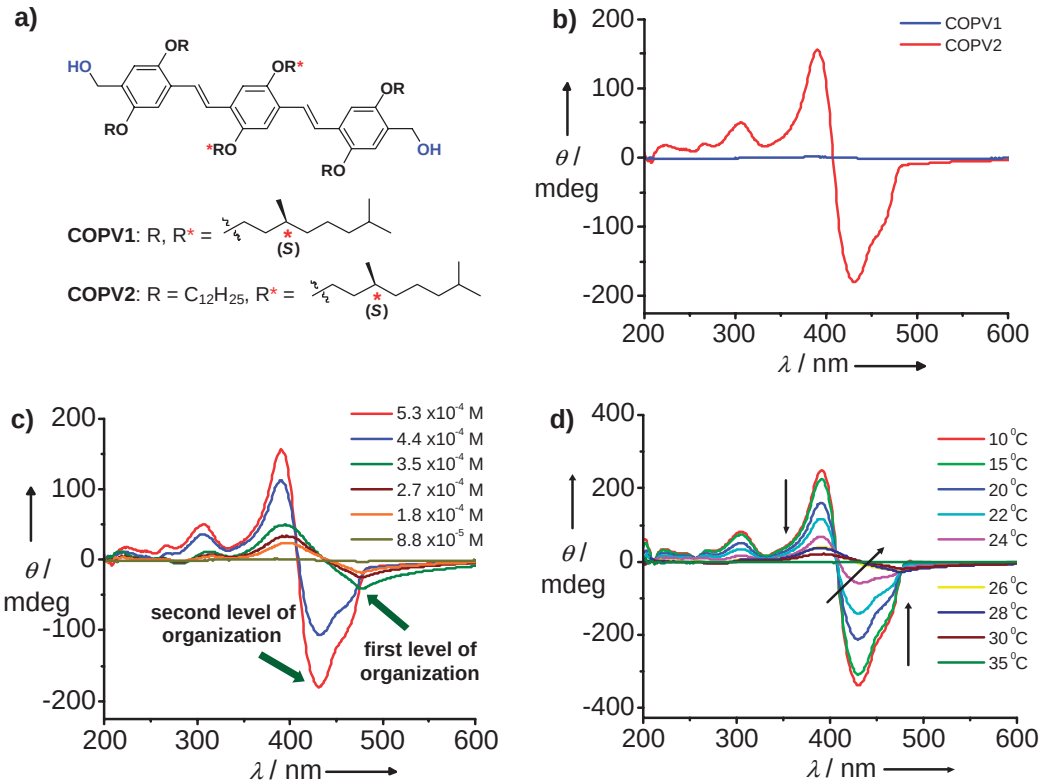

Figure 7. (a) Molecular structure of chiral OPVs. (b) CD spectra of chiral OPVs in dodecane (5.3×10^{-4} M). (c) Concentration- and (d) temperature-dependent CD spectra of COPV**2** (5.3×10^{-4} M) in dodecane. Reprinted from Ref. 23 with permission. Copyright 2004 Wiley-VCH.

having two chiral side chains on the middle benzene moiety forms gels in aliphatic hydrocarbon solvents at higher concentrations (>6 mM). This observation indicates that the branched chiral side chain considerably reduces the gelation ability of OPVs. Absorption and emission studies of chiral OPVs in dodecane revealed that COPV**1** exists as monomeric species irrespective of the concentrations, whereas COPV**2** showed a greater tendency to form aggregates. CD experiments revealed the absence of CD response for COPV**1**. However, COPV**2** (5.3×10^{-4} M) exhibited a strong bisignate Cotton effect at the position of the π–π^* transition, with a zero crossing close to the absorption maximum at 400 nm (Figure 7b). The exciton coupled bisignate negative couplet in the CD spectrum is a signature of the left-handed helical assembly of COPV**2** that specify that the chiral side chains account for a bias of helicity by transferring the chiral information to the self-assembled chromophores.

Detailed concentration and temperature-dependent CD studies of COPV**2** in dodecane indicated the CD signal transition during the hierarchical growth of the initially formed chiral assemblies into helical fibers and coiled-coil ropes. The CD spectral changes between 8.8×10^{-5} to 5.3×10^{-4} M concentration range at 20 °C is shown in Figure 7c. Up to a concentration of 2.7×10^{-4} M, COPV**2** in dodecane showed a bisignate CD signal with a negative first Cotton effect followed by a second positive Cotton effect with a zero crossing around 440 nm, which is not on the absorption maximum of the chromophore. Surprisingly, above 3.5×10^{-4} M concentration, a sharp transition of the CD signal could be seen with a zero crossing exactly at the absorption maximum (400 nm). Temperature-dependent study at a concentration of 5.3×10^{-4} M in dodecane showed a decrease in the CD signal up to a temperature of 24 °C along the zero crossing point (Figure 7d). However at 26 °C, a sharp transition of the intense exciton-coupled CD signal to a weak bisignate signal with a shift of the zero crossing from 400–440 nm was noted, which continued to decrease till it reached the baseline at 35 °C. In the initial levels, the molecules organize to form left-handed chiral aggregates, which are helical as indicated by the weak bisignate CD signal. At higher concentrations, these initial chiral assemblies grow further into helical fibers and coiled-coil ropes, thus resulting in a strong exciton-coupled CD signal. Based on the CD and the morphological evidence, the helical assembly of COPV**2** to helical ropes is represented as shown in Figure 8.

5. Chirality Amplification: The Sergeants and Soldiers Effect in OPV Self-Assemblies

Chirality induction via "sergeants and soldiers" approach has been extensively used to the design of helical polymers and supramolecular systems.[3c,4,24] Recently, we have illustrated this approach to induce helicity using gel forming chiral (COPV**2**, sergeants) and achiral OPVs (OPV**2**, soldiers).[25] COPV**2** form left-handed (M) helical assembly in dodecane as deduced from CD studies (Figure 7). Further confirmation is obtained from the AFM analysis, which showed the formation of M-helical fibers having width in the range of 78–176 nm and length in several micrometers (Figure 9a). AFM

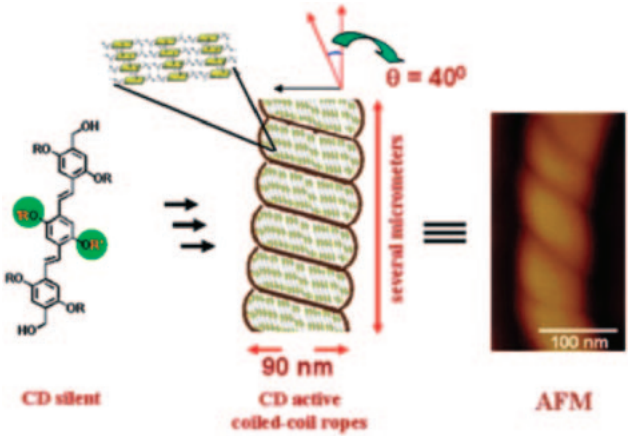

Figure 8. Representation of the hierarchical self-assembly of COPV**2** to coiled-coil helical nanostructures. AFM image of a coiled-coil rope is shown on the right. Reprinted from Ref. 23 with permission. Copyright 2004 Wiley-VCH.

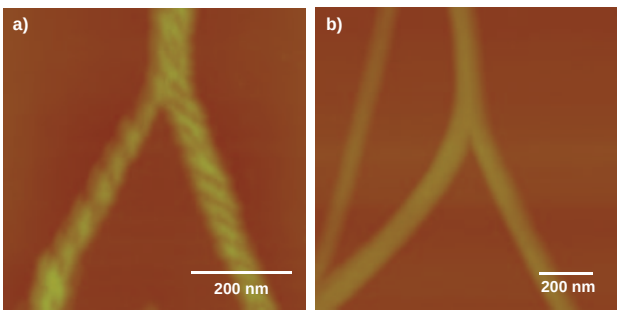

Figure 9. AFM height images of (a) COPV**2** and (b) OPV**2** in dodecane (9×10^{-5} M) on freshly cleaved mica by drop-casting under ambient conditions.

analysis of the corresponding achiral OPV**2** showed the formation of nonhelical supramolecular tapes with width in the range of 100–250 nm and length in several micrometers (Figure 9b). However, co-assembly of OPV**2** and COPV**2** revealed a composition dependent change in the helical bias as confirmed by the CD and AFM analyses.

At very low mol % of COPV**2**, the coassembly exhibited an inverted CD signal with a near mirror image relationship. Intensity of the CD signal increased with increase in the composition of COPV**2** up to 22 mol % (Figure 10a). Above 22 mol %, the intensity of the CD signal was decreased with a gradual blue shift of the positive Cotton signal, which tends to move towards the native CD of COPV**2** (Figure 10e). AFM analysis of the coassembly at different mol % of COPV**2** showed the formation of right-handed (P) helices along with a few left-handed (M) helices at 9 mol % of COPV**2** (Figure 10b). The smallest P-helix observed had a width of 106 nm with an almost uniform pitch of 200 nm. The number of M-helices increased with increase in the composition of COPV**2**. At 60 mol %, the AFM image revealed the presence of M-helices with a few P-helices (Figure 10f). In addition to the individually biased M- and P-helices, longitudinally fused left- and right-handed helices were also observed. Such unusual structures were observed in large number at 20 mol % of COPV**2** (Figure 10d). At this composition, a dramatic change in the CD signal is observed. Insight from the CD and AFM analyses revealed that a change in the helical bias of the supramolecular chirality is possible within the OPV assemblies without changing the chiral handle attached to the chromophores. It is interesting to note that in the "sergeants and soldiers" approach reported previously, the soldiers strictly follow the instructions of the chiral sergeants.[24] In the present case, however, at low mol % of the sergeants, the soldiers mistake orders from the former and behave in an opposite sense, which is not commonly observed in co-assembled supramolecular architectures.

6. Self-Assembly of Cholesterol-Tethered OPV Derivatives: Twisted and Coiled Helices

Functionalization of OPV**2** with cholesterol, a naturally occurring chiral motif resulted in an unprecedented control on the arrangements of the molecules in the supramolecular assembly.[26,27] A striking difference between the mono- and bis-cholesterol-functionalized OPV derivatives (OPV**3** and OPV**4** respectively) is the disparity in the gelation behavior. Although both compounds induce the gelation of a variety of hydrocarbon solvents, gels formed from OPV**4** were found to be relatively weaker than those with OPV**3**. The critical gelator concentration (CGC) of OPV**4** in decane is 7.0 mM whereas that of OPV**3** is only 3.4 mM, which is nearly twofold less. The melting transition of the gel (T_{gel}) showed a higher value for OPV**3** gels when compared to that of OPV**4** at similar concentrations in decane. In addition, the presence of cholesterol moiety substantially altered the helical packing of OPV derivatives which is clear from the optical, chiroptical, and morphological studies. For example, the mono-cholesterol-functionalized OPV (OPV**3**) showed broad absorption and emission spectra upon self-assembly whereas the bis-cholesterol-functionalized OPV (OPV**4**) exhibited structured absorption and emission. The gel with OPV**3** showed a weak yellow emission whereas the gel from OPV**4** displayed a relatively strong green emission, indicating differences in the electronic properties of the self-assemblies.

In chloroform solutions, OPV**3** and OPV**4** did not show CD response (Figure 11). However, OPV**4** in decane (3×10^{-4} M) showed an exciton-coupled bisignate CD signal with negative ($\lambda_{max} = 418$ nm) and positive ($\lambda_{max} = 385$ nm) Cotton effects, which change sign exactly through the π–π^* absorption maximum at 398 nm (Figure 11b). This behavior is characteristic of a left-handed helical bias of the supramolecular chirality. In the case of OPV**3**, the CD spectrum in decane showed a strange behavior with a first positive ($\lambda_{max} = 393$ nm) followed by two negative ($\lambda_{max} = 308$ and 269 nm) Cotton signals (Figure 11a). The non-bisignate exciton couplet with opposite signals indicates the possibility of different chiral aggregates. Furthermore, the measure of chirality (g) for OPV**3** is low ($g_{393\,nm} = 5.2 \times 10^{-4}$) relative to that of OPV**4** ($g_{385\,nm} = 9.3 \times 10^{-4}$) which indicates a weak exciton coupling in the former. These differences in the CD spectra reiterate the differences between the aggregates of OPV**3** and OPV**4** and agree with the absorption and emission spectral changes.

AFM textures of OPV**3** and OPV**4** obtained from solutions in decane showed significant differences, although both assem-

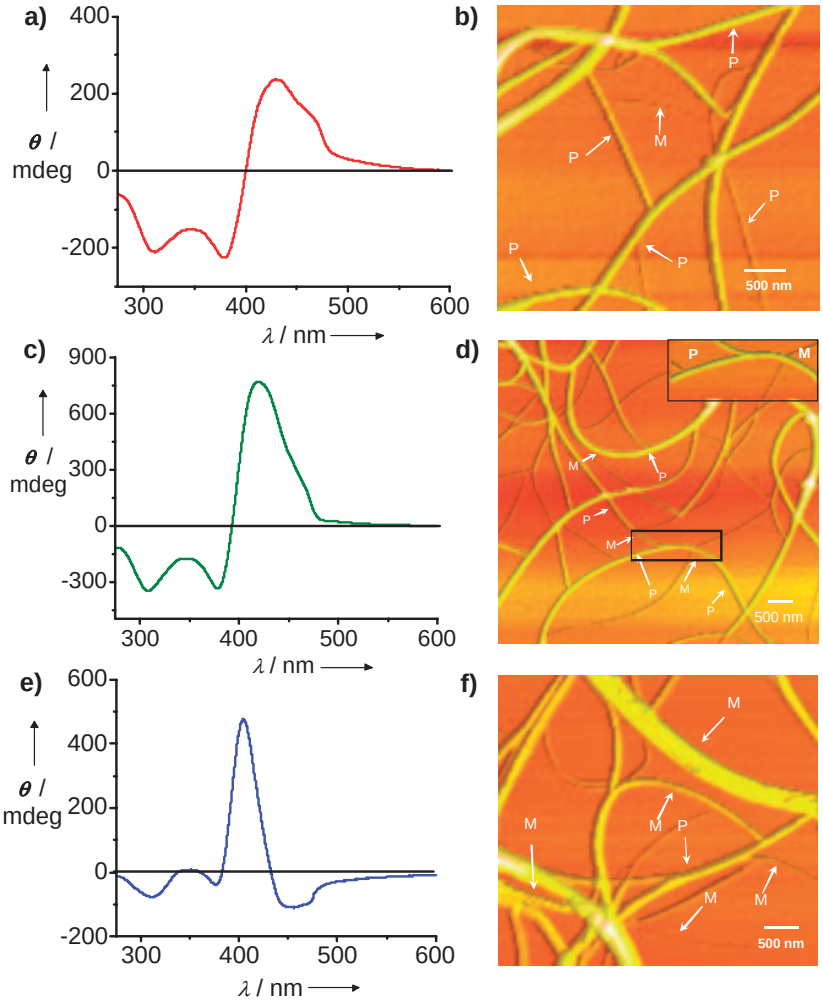

Figure 10. CD spectra and the corresponding AFM height images of co-assembled OPV**1** with (a, b) 9 mol %, (c, d) 20 mol %, and (e, f) 60 mol % of COPV**2**. The inset of Figure 10d shows zoomed image of marked area which shows formation of fused helices at 20 mol % of COPV**2**. AFM samples were prepared in dodecane (9×10^{-5} M) and transferred to freshly cleaved mica by drop-casting under ambient conditions. Reprinted from Ref. 25 with permission. Copyright 2006 Wiley-VCH.

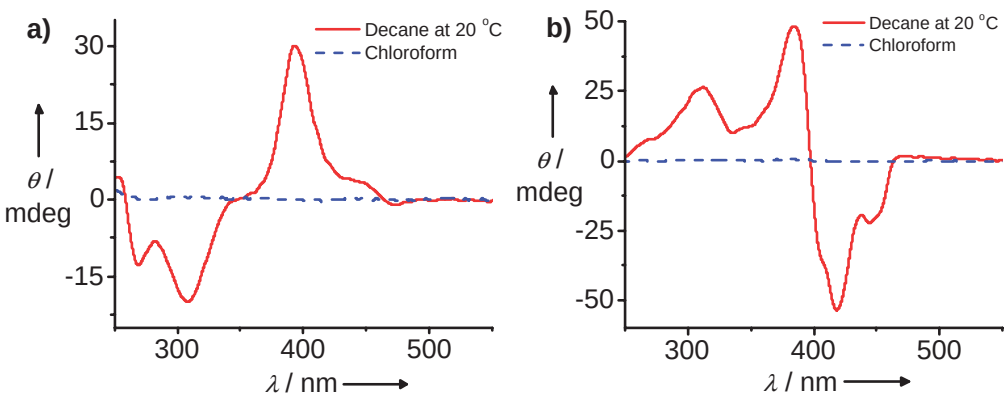

Figure 11. CD spectra of (a) OPV**3** and (b) OPV**4** in chloroform and decane (3×10^{-4} M). Reprinted from Ref. 26 with permission. Copyright 2006 Wiley-VCH.

blies adopt right-handed (P) helical structures (Figure 12). The helicity of OPV**3** is in agreement with the CD spectrum, whereas that of OPV**4** disagrees with the bisignate CD signal. Such a contradiction of the observed CD and morphological features has previously been reported (Figure 11 and Figure 12).[28] In many cases, the initially formed 1D aggregates with a left-handed twist may wind in the opposite direction during the formation of hierarchical assembly resulting in ultimate

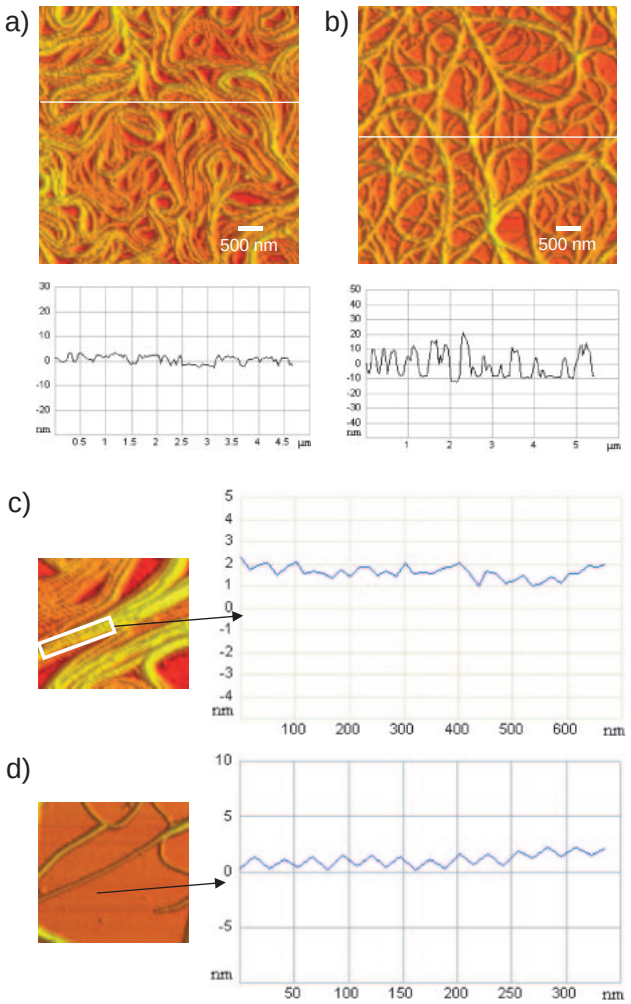

Figure 12. AFM images of (a) OPV**3** and (b) OPV**4** with the corresponding height profiles. (c and d) Zoomed region of the self-assembled OPV**3** and OPV**4** respectively, with the corresponding section analyses. Samples were prepared from solutions in decane (1×10^{-5} M) and transferred to freshly cleaved mica sheet by drop-casting. Reprinted from Ref. 26 with permission. Copyright 2006 Wiley-VCH.

right-handed twist, as can be seen to some extent in some of the large fibers of OPV**4**. AFM analysis reveals ribbon-like structures of OPV**3** that are flat and aligned sideways to form coiled superstructures (Figure 12a). The width of the individual ribbons varies from 30–70 nm, with an average height of 4–8 nm. The height of 8 nm corresponds to two individual tapes lying one over the other. Interestingly, OPV**4** showed branched helical fibers of different sizes which are entangled to form a network structure (Figure 12b). The width of the smallest fiber is 40 nm, with a height of 4 nm and is several micrometers in length. The height profiles of wide areas of the samples showed a uniform height for OPV**3**, whereas a height variation of 4–50 nm was observed for OPV**4**. Furthermore, section analysis along the axis (Figures 12c and 12d) revealed that assemblies of OPV**3** have an irregular helical pitch of 40–80 nm whereas those of OPV**4** are almost uniform with zigzag patterns and have a pitch length of 46 nm. Irregular movements of the AFM tip through the long axis of the assembly with variable pitch length and uniform height profile are characteristic of a flexible and flattened coiled tape like morphology of OPV**3**. In contrast, the uniform zigzag patterns along the axis and variable height profiles of OPV**4** are characteristic of twisted helical fibrillar assemblies of different size that are intertwined.

On the basis of the differences in the optical, chiroptical, gelation and morphological properties, it is clear that the packing of the individual molecules in their respective supramolecular assemblies are different. The optical and chiroptical features strongly support a well-organized twisted helical arrangement of the molecules in the bis-cholesterol derivative and a hydrogen-bond assisted tilted arrangement in the mono-cholesterol derivative (Figure 13). The extended supramolecular assembly of the twisted packing (pseudo-H aggregates) leads to twisted helical assemblies, whereas the tilted packing (pseudo-J aggregates) results in a coiled helical assembly. Although there are several reports on the formation of helical supramolecular structures of rigid chromophoric systems, this is a unique example that illustrate the formation of helical assemblies with distinct morphological, optical, and chiroptical behavior. It is worth mentioning here that the difference in the optical properties could be derived without altering the conjugation length or the electron donor–acceptor strength of the individual molecules. The difference in the packing of the molecules in a hierarchical self-assembly is sufficient enough to produce large variations in the electronic properties.

7. Self-Assembly of Oligo(*p*-phenyleneethynylene)s (OPEs): Spherical and Helical Assemblies

Self-assembly of oligo- and poly(*p*-phenyleneethynylene)s has been extensively studied in mixed solvents of different polarities.[29,30] However, not much attention has been paid to the self-assembly and gelation of para linked short OPEs in a single solvent of choice. Keeping this in view, we have synthesized a few OPE derivatives (Chart 5) and studied their self-assembly behavior using spectroscopic and microscopic techniques.[31]

The absorption spectrum of OPE**1** in decane (1.1×10^{-5} M) showed the π–π^* band at 387 nm with a shoulder at 419 nm which indicates the aggregation of OPE**1** under this condition. Temperature-dependent absorption studies of OPE**1** in decane showed a transition from the aggregate to the molecularly dissolved species in between 20–70 °C (Figure 14a). A plot of the fraction of aggregates (α) versus temperature revealed two types of transitions indicating the presence of aggregates of different thermal stabilities (Figure 14a inset). Furthermore, the room-temperature absorption spectrum of OPE**1** in decane showed a time-dependent decreases of absorption intensity leading to a broad spectrum (Figure 14b). The time-dependent change in the absorption spectrum reached a stable state after 6 h. These observations indicate the initial formation of kinetically controlled aggregated species, which undergoes a slow transformation into thermodynamically stable aggregates (Figure 14b inset).[31a]

To understand more about the morphology of these aggregates, we have carried out detailed studies using AFM, TEM, SEM, and optical microscopy.[31a] AFM analysis of

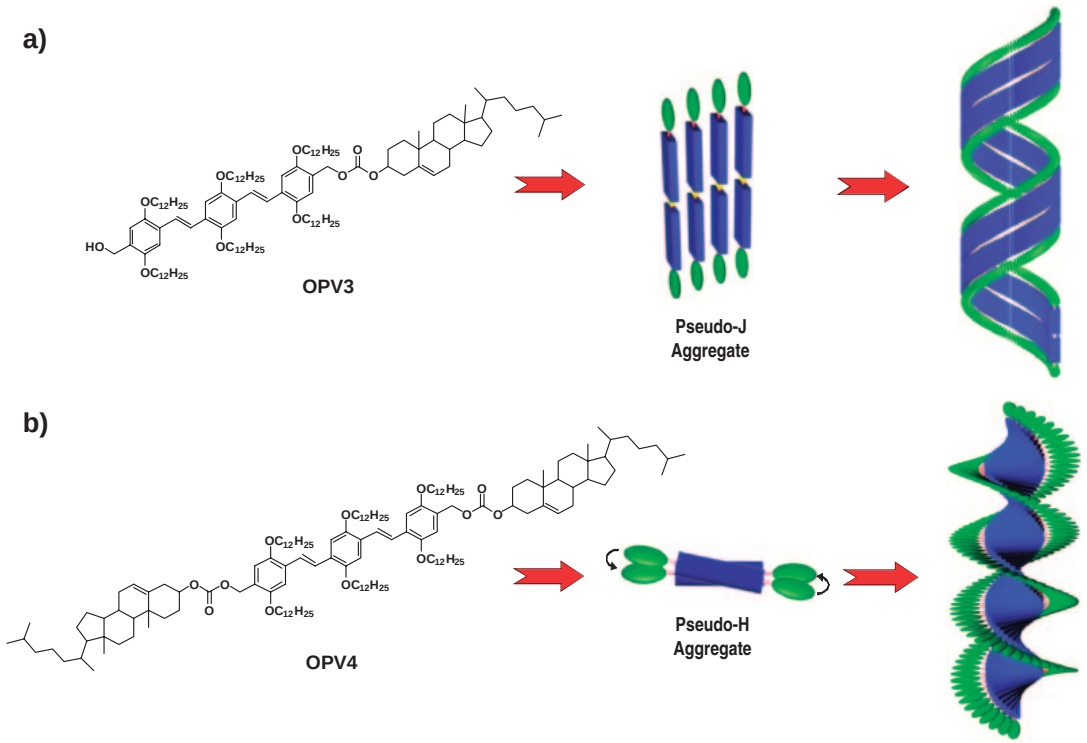

Figure 13. Probable mode of molecular packing in the self-assembly of cholesterol appended OPV derivatives in decane. (a) OPV**3** and (b) OPV**4**. Reprinted from Ref. 26 with permission. Copyright 2006 Wiley-VCH.

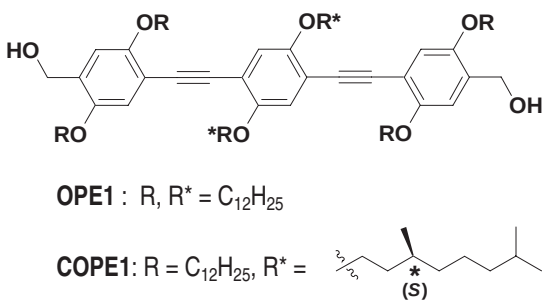

Chart 5.

OPE**1** in decane showed the formation of nanospheres having different diameter and height. For example, at a concentration of 1×10^{-6} M, flattened nanospheres with an average diameter of 94 ± 2 nm and a height of 4 ± 1 nm were formed (Figure 15a). Increase in concentration of OPE**1** to 1×10^{-5} M resulted in the formation of spheres with increased diameter and height. Moreover, these spherical aggregates are found to be vesicular in nature as evident from the TEM analysis that showed a significant contrast difference between the inner and the periphery (Figure 15b). The wall thickness of the vesicles is estimated approximately as 10 nm with bilayer morphology, each layer having a thickness of 4 nm. Optical microscopic studies at a concentration of 1×10^{-4} M showed the formation of microspheres of 5–10 μm in diameter with strong blue fluorescence. Interestingly, when the concentration of the solution was increased to 3.5×10^{-3} M, a self-supporting gel with blue fluorescence was observed. SEM analysis of the gel revealed the formation of micrometer sized extended superstructures. XRD pattern of the dried gel indicated a lamellar packing of the molecules. This study provides a simple method to prepare stable spherical and extended self-assemblies of OPEs with different size and shape from a single solvent.

The sergeants and soldiers experiment with OPE**1** and COPE**1** showed formation of helical tubules instead of vesicles during the coassembly.[31b] Optical and chiroptical studies revealed that COPE**1** is not able to form aggregates in decane. AFM analysis of COPE**1** from decane showed the formation ill-defined aggregates. This behavior of COPE**1** is significantly different from the corresponding OPV derivative, which forms left-handed helical tapes and gels in decane. As expected, OPE**1** was CD silent, since the molecule is achiral. However, addition of COPE**1** (5–30 mol %) to a solution of OPE**1** (1×10^{-5} M) in decane, followed by heating and cooling, resulted in a positive Cotton signal and two negative signals (Figure 16a). Since, both individual components are CD-silent, the observed CD of the co-assembly is due to the induced chirality from COPE**1** in a helical sense. The intensity of the induced CD (ICD) signals increases with increasing fraction of COPE**1** up to 30 mol %, then decreases, and finally disappears at 50 mol %, which is clear from the plots of the ICD intensity at 420 nm against the concentration of COPE**1** (Figure 16b). The increase in the ICD intensity reveals that up to 30 mol % COPE**1** is able to induce chirality in OPE**1**. Above this concentration, co-assembly is destabilized, as indicated by the decreased CD intensity, which finally disappears at higher concentrations of COPE**1** (50 mol %).

AFM pictures of the co-assemblies of COPE**1** with OPE**1** revealed the formation of both nanoparticles and helical structures at 8 mol % of the former (Figure 17a). The width of the particles obtained under these conditions varies in the range

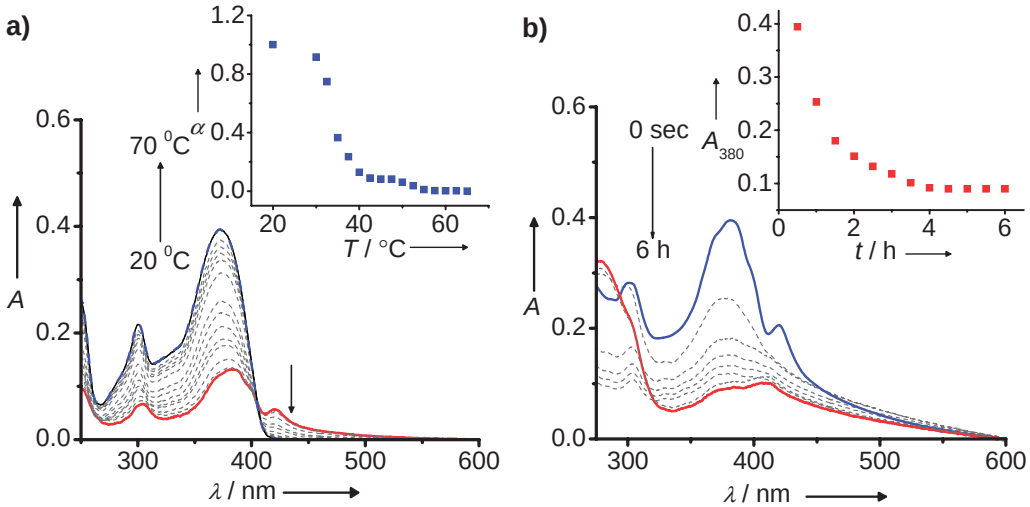

Figure 14. (a) Temperature- and (b) time-dependent absorption changes of OPE**1** in decane (1.1×10^{-5} M). The insets show (a) the plot of the fraction of aggregates (α) versus temperature (absorption monitored at 380 nm) and (b) the changes in the absorbance at 380 nm versus time. Reprinted from Ref. 31a with permission. Copyright 2006 Wiley-VCH.

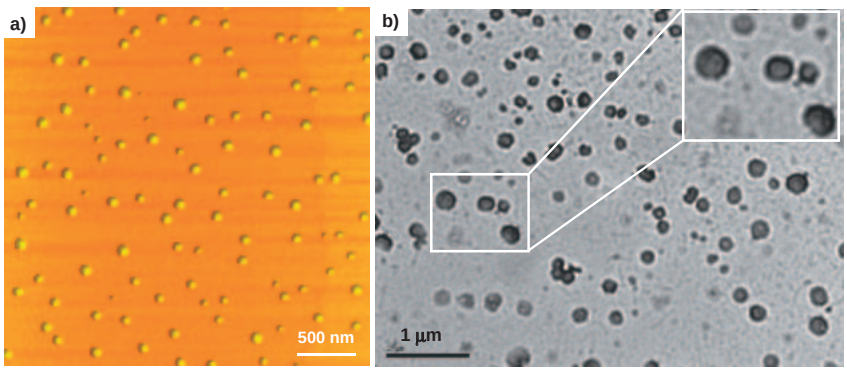

Figure 15. (a) Tapping-mode AFM height and (b) TEM images of OPE**1** from decane (1×10^{-6} M). The inset shows zoomed portion of the marked area. Reprinted from Ref. 31b with permission. Copyright 2006 Wiley-VCH.

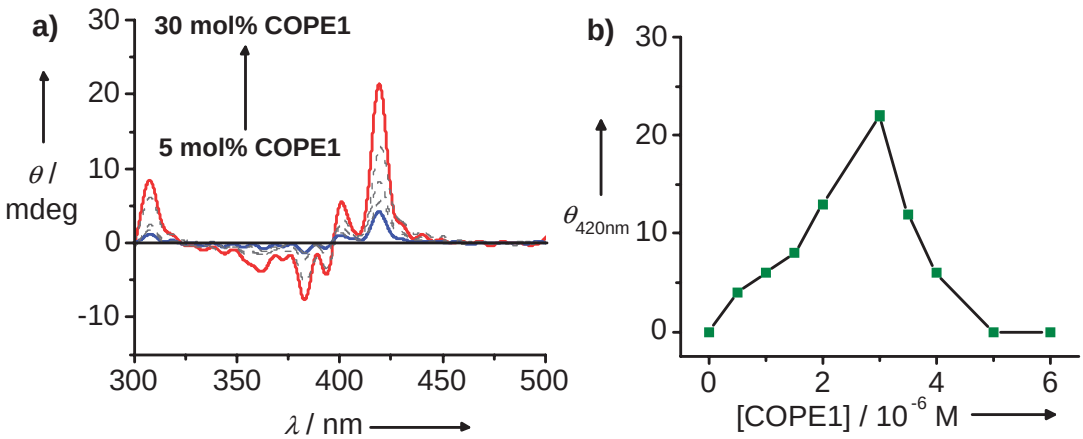

Figure 16. (a) CD spectra of OPE**1** with different fractions of added COPE**1** in decane (1×10^{-5} M). (b) Plots of CD intensity at 420 nm against concentration of COPE**1**. Reprinted from Ref. 31b with permission. Copyright 2006 Wiley-VCH.

of 30–60 nm with average heights of 3–16 nm. However, at 25 mol % of COPE**1** almost all the spherical assemblies were transformed into helical structures (Figure 17b). Section analysis of the helical fibers revealed a width of 90 nm for the smallest fiber with almost uniform pitch of 140 nm. The height of the fibers varies between 6 and 25 nm, which indicates considerable flattening of the fibers. However, TEM analysis of the co-assembly revealed that the helical fibers are tubular in

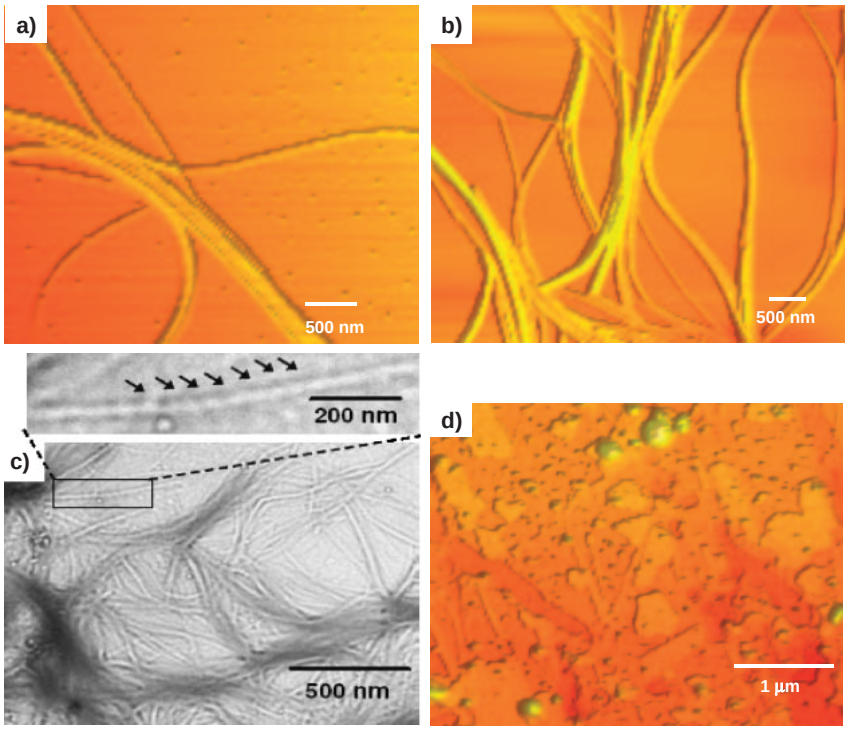

Figure 17. Tapping-mode AFM height images of the co-assembly of OPE**1** with different concentrations of COPE**1** from decane (1×10^{-5} M). (a) 8, (b) 25, and (d) 50 mol % under ambient conditions on freshly cleaved mica surface (z scale = 50 nm). (c) TEM images (unstained) of 25 mol % COPE**1** with OPE**1** under ambient conditions. The inset is a zoomed image of the marked area showing the helical-tubular nature of the co-assembly. Reprinted from Ref. 31b with permission. Copyright 2006 Wiley-VCH.

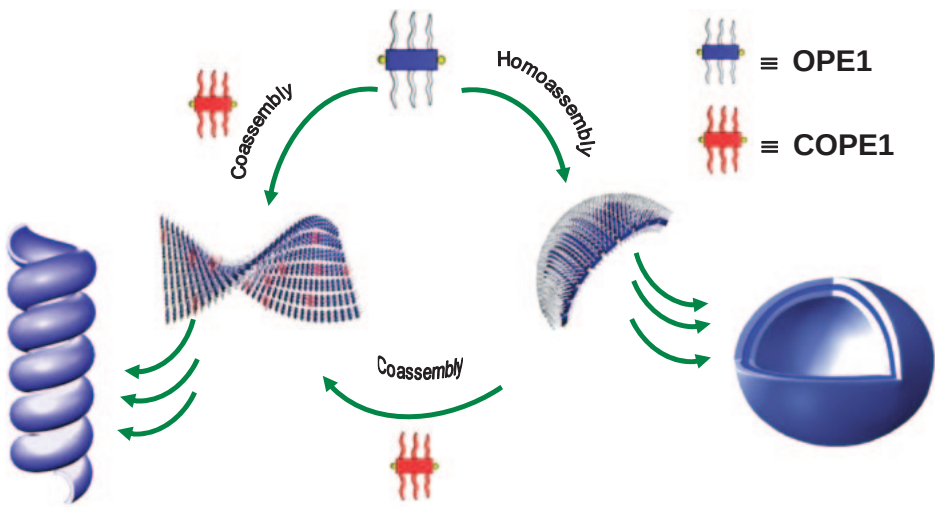

Figure 18. Self-assembly of OPE**1** to vesicles and subsequent transformation into helical tubes upon co-assembly with COPE**1** in decane. Reprinted from Ref. 31b with permission. Copyright 2006 Wiley-VCH.

nature with diameters of 55–90 nm (Figure 17c). The width of the inner hollow tubular space is almost uniform in all cases. Moreover, at high concentration of COPE**1** (>50 mol %), complete disappearance of the helical structures was observed which is in agreement with the chiroptical studies (Figure 17d). These results indicate that although COPE**1** alone is unable to form self-assemblies, it facilitate the co-assembly formation with OPE**1**. During this process, COPE**1** transfers the chiral information to the self-assembly thereby controlling the morphology from vesicular to helical tubular assemblies (Figure 18).

8. Conclusion and Outlook

In summary, we have highlighted the self-assembly of OPVs and OPEs along with a few other related systems that form different supramolecular architectures such as nanotapes, helices, vesicles, and helical tubules, leading to gel formation under appropriate conditions. Incorporation of chiral handles

allows the formation of helical assemblies of OPVs whereas analogous OPEs with chiral handles failed to form self-assemblies. Interestingly, in both cases, co-assembly with achiral derivatives induces and amplifies the molecular chirality of the chiral component leading to supramolecular helical architectures. Noticeably, OPVs exhibit high sensitivity towards the morphological, optical, and chiroptical properties. Structural variations in OPVs, as in mono- and bis-cholesterol derivatives, show significant role in controlling the morphology of the resultant helical structures. The difference in the strength of π-stacking in OPVs and OPEs are detrimental in the observed morphology differences between the two systems.

A.A. thanks the Department of Science and Technology (DST) for financial support under the Nanoscience and Technology Initiatives and for a Ramanna Fellowship. Support under the network programme of the Council of Scientific and Industrial Research (CSIR) is acknowledged. V. K. P., S. S. B., C. V., and R. V. are grateful to CSIR for research fellowships. This is contribution no. NIIST-PPG-269

References

1 a) A. E. Rowan, R. J. M. Nolte, *Angew. Chem., Int. Ed.* **1998**, *37*, 63. b) C. Schmuck, *Angew. Chem., Int. Ed.* **2003**, *42*, 2448. c) P. Cintas, *Angew. Chem., Int. Ed.* **2007**, *46*, 4016.

2 a) J. J. L. M. Cornelissen, A. E. Rowan, R. J. M. Nolte, N. A. J. M. Sommerdijk, *Chem. Rev.* **2001**, *101*, 4039. b) L. Brunsveld, B. J. B. Folmer, E. W. Meijer, R. P. Sijbesma, *Chem. Rev.* **2001**, *101*, 4071. c) L. Pérez-García, D. B. Amabilino, *Chem. Soc. Rev.* **2002**, *31*, 342.

3 a) M. A. Mateos-Timoneda, M. Crego-Calama, D. N. Reinhoudt, *Chem. Soc. Rev.* **2004**, *33*, 363. b) A. Brizard, R. Oda, I. Huc, *Top. Curr. Chem.* **2005**, *256*, 167. c) A. R. A. Palmans, E. W. Meijer, *Angew. Chem., Int. Ed.* **2007**, *46*, 8948. d) H.-J. Kim, Y.-B. Lim, M. Lee, *J. Polym. Sci., Part A: Polym. Chem.* **2008**, *46*, 1925.

4 a) M. M. Green, J.-W. Park, T. Sato, A. Teramoto, S. Lifson, R. L. B. Selinger, J. V. Selinger, *Angew. Chem., Int. Ed.* **1999**, *38*, 3138. b) M. M. Green, K.-S. Cheon, S.-Y. Yang, J.-W. Park, S. Swansburg, W. Liu, *Acc. Chem. Res.* **2001**, *34*, 672. c) E. Yashima, K. Maeda, T. Nishimura, *Chem.—Eur. J.* **2004**, *10*, 42.

5 a) *Circular Dichroism: Principles and Applications*, 4th ed., ed. by N. Berova, K. Nakanishi, R. W. Woody, Wiley-VCH, Weinheim, **2000**. b) *Materials-Chirality*: *Vol. 24 of Topics in Stereochemistry*, ed. by M. M. Green, R. J. M. Nolte, E. W. Meijer, John Wiley & Sons, Inc., Hoboken, New Jersey, **2003**. c) *Supramolecular Chirality: Vol. 265 of Topics in Current Chemistry*, ed. by M. Crego-Calama, D. N. Reinhoudt, Springer-Verlag, Berlin, Heidelberg, **2006**.

6 a) Y. Okamoto, T. Nakano, *Chem. Rev.* **1994**, *94*, 349. b) H. Ogoshi, T. Mizutani, *Acc. Chem. Res.* **1998**, *31*, 81. c) B. L. Feringa, R. A. van Delden, N. Koumura, E. M. Geertsema, *Chem. Rev.* **2000**, *100*, 1789. d) I. Stibor, P. Zlatušková, *Top. Curr. Chem.* **2005**, *255*, 31. e) G. A. Hembury, V. V. Borovkov, Y. Inoue, *Chem. Rev.* **2008**, *108*. 1. f) H. Tanaka, S. Matile, *Chirality* **2008**, *20*, 307. g) Y. Shoji, K. Tashiro, T. Aida, *Chirality* **2008**, *20*, 420.

7 a) M. van der Auweraer, F. C. De Schryver, *Nat. Mater.* **2004**, *3*, 507. b) A. P. H. J. Schenning, E. W. Meijer, *Chem. Commun.* **2005**, 3245.

8 a) F. J. M. Hoeben, P. Jonkheijm, E. W. Meijer, A. P. H. J. Schenning, *Chem. Rev.* **2005**, *105*, 1491. b) *Supramolecular Dye Chemistry: Vol. 258 of Topics in Current Chemistry*, ed. by F. Würthner, Springer-Verlag, Berlin, Heidelberg, **2005**. c) A. C. Grimsdale, K. Müllen, *Angew. Chem., Int. Ed.* **2005**, *44*, 5592.

9 Two recent reports on supramolecular assemblies show linear dichroism (LD) effects as a result of convective flow (shaking or stirring) and resultant alignment of the fibers in the cuvette. Such LD effects may contribute to the apparent CD spectra of self-assemblies: a) A. Tsuda, M. A. Alam, T. Harada, T. Yamaguchi, N. Ishii, T. Aida, *Angew. Chem., Int. Ed.* **2007**, *46*, 8198. b) M. Wolffs, S. J. George, Ž. Tomović, S. C. J. Meskers, A. P. H. J. Schenning, E. W. Meijer, *Angew. Chem., Int. Ed.* **2007**, *46*, 8203.

10 a) A. P. H. J. Schenning, P. Jonkheijm, E. Peeters, E. W. Meijer, *J. Am. Chem. Soc.* **2001**, *123*, 409. b) P. Jonkheijm, F. J. M. Hoeben, R. Kleppinger, J. van Herrikhuyzen, A. P. H. J. Schenning, E. W. Meijer, *J. Am. Chem. Soc.* **2003**, *125*, 15941. c) P. Jonkheijm, P. van der Schoot, A. P. H. J. Schenning, E. W. Meijer, *Science* **2006**, *313*, 80.

11 P. Jonkheijm, A. Miura, M. Zdanowska, F. J. M. Hoeben, S. De Feyter, A. P. H. J. Schenning, F. C. De Schryver, E. W. Meijer, *Angew. Chem., Int. Ed.* **2004**, *43*, 74.

12 a) R. Iwaura, F. J. M. Hoeben, M. Masuda, A. P. H. J. Schenning, E. W. Meijer, T. Shimizu, *J. Am. Chem. Soc.* **2006**, *128*, 13298. b) P. G. A. Janssen, J. Vandenbergh, J. L. J. van Dongen, E. W. Meijer, A. P. H. J. Schenning, *J. Am. Chem. Soc.* **2007**, *129*, 6078. c) S. J. George, Z. Tomović, M. M. J. Smulders, T. F. A. de Greef, P. E. L. G. Leclère, E. W. Meijer, A. P. H. J. Schenning, *Angew. Chem., Int. Ed.* **2007**, *46*, 8206.

13 a) J.-H. Fuhrhop, T. Wang, *Chem. Rev.* **2004**, *104*, 2901. b) J.-H. Ryu, D.-J. Hong, M. Lee, *Chem. Commun.* **2008**, 1043. c) Y.-b. Lim, K.-S. Moon, M. Lee, *J. Mater. Chem.* **2008**, *18*, 2909.

14 a) P. Jonkheijm, M. Fransen, A. P. H. J. Schenning, E. W. Meijer, *J. Chem. Soc., Perkin Trans. 2* **2001**, 1280. b) F. J. M. Hoeben, I. O. Shklyarevskiy, M. J. Pouderoijen, H. Engelkamp, A. P. H. J. Schenning, P. C. M. Christianen, J. C. Maan, E. W. Meijer, *Angew. Chem., Int. Ed.* **2006**, *45*, 1232.

15 a) A. F. M. Kilbinger, A. P. H. J. Schenning, F. Goldoni, W. J. Feast, E. W. Meijer, *J. Am. Chem. Soc.* **2000**, *122,* 1820. b) A. P. H. J. Schenning, A. F. M. Kilbinger, F. Biscarini, M. Cavallini, H. J. Cooper, P. J. Derrick, W. J. Feast, R. Lazzaroni, Ph. Leclère, L. A. McDonell, E. W. Meijer, S. C. J. Meskers, *J. Am. Chem. Soc.* **2002**, *124*, 1269.

16 S.-i. Kawano, N. Fujita, S. Shinkai, *Chem.—Eur. J.* **2005**, *11*, 4735.

17 a) J. Bae, J.-H. Choi, Y.-S. Yoo, N.-K. Oh, B.-S. Kim, M. Lee, *J. Am. Chem. Soc.* **2005**, *127*, 9668. b) J.-H. Ryu, H.-J. Kim, Z. Huang, E. Lee, M. Lee, *Angew. Chem., Int. Ed.* **2006**, *45*, 5304.

18 a) J. Gierschner, J. Cornil, H.-J. Egelhaaf, *Adv. Mater.* **2007**, *19*, 173. b) H. Meier, *Angew. Chem., Int. Ed.* **2005**, *44*, 2482. c) J. L. Segura, N. Martín, *J. Mater. Chem.* **2000**, *10*, 2403. d) *Electronic Materials: The Oligomer Approach*, ed. by K. Müllen, G. Wegner, Wiley-VCH, Weinheim, **1998**.

19 a) A. Ajayaghosh, S. J. George, A. P. H. J. Schenning, *Top. Curr. Chem.* **2005**, *258*, 83. b) A. Ajayaghosh, V. K. Praveen, *Acc. Chem. Res.* **2007**, *40*, 644. c) A. Ajayaghosh, V. K. Praveen, C. Vijayakumar, *Chem. Soc. Rev.* **2008**, *37*, 109.

20 a) A. Ajayaghosh, S. J. George, *J. Am. Chem. Soc.* **2001**, *123*, 5148. b) S. J. George, A. Ajayaghosh, *Chem.—Eur. J.*

2005, *11*, 3217. c) R. Varghese, S. J. George, A. Ajayaghosh, *Chem. Commun.* **2005**, 593. d) V. K. Praveen, S. J. George, A. Ajayaghosh, *Macromol. Symp.* **2006**, *241*, 1.

21 a) B. W. Messmore, J. F. Hulvat, E. D. Sone, S. I. Stupp, *J. Am. Chem. Soc.* **2004**, *126*, 14452. b) J. F. Hulvat, M. Sofos, K. Tajima, S. I. Stupp, *J. Am. Chem. Soc.* **2005**, *127*, 366. c) S. Yagai, S. Kubota,T. Iwashima, K. Kishikawa, T. Nakanishi, T. Karatsu, A. Kitamura, *Chem.—Eur. J.* **2008**, *14*, 5246.

22 a) A. Ajayaghosh, S. J. George, V. K. Praveen, *Angew. Chem., Int. Ed.* **2003**, *42*, 332. b) A. Ajayaghosh, C. Vijayakumar, V. K. Praveen, S. S. Babu, R. Varghese, *J. Am. Chem. Soc.* **2006**, *128*, 7174. c) V. K. Praveen, S. J. George, R. Varghese, C. Vijayakumar, A. Ajayaghosh, *J. Am. Chem. Soc.* **2006**, *128*, 7542. d) A. Ajayaghosh, V. K. Praveen, S. Srinivasan, R. Varghese, *Adv. Mater.* **2007**, *19*, 411. e) A. Ajayaghosh, V. K. Praveen, C. Vijayakumar, S. J. George, *Angew. Chem., Int. Ed.* **2007**, *46*, 6260.

23 S. J. George, A. Ajayaghosh, P. Jonkheijm, A. P. H. J. Schenning, E. W. Meijer, *Angew. Chem., Int. Ed.* **2004**, *43*, 3422.

24 a) L. J. Prins, P. Timmerman, D. N. Reinhoudt, *J. Am. Chem. Soc.* **2001**, *123*, 10153. b) R. B. Prince, J. S. Moore, L. Brunsveld, E. W. Meijer, *Chem.—Eur. J.* **2001**, *7*, 4150. c) A. J. Wilson, M. Masuda, R. P. Sijbesma, E. W. Meijer, *Angew. Chem., Int. Ed.* **2005**, *44*, 2275. d) W. Jin, T. Fukushima, M. Niki, A. Kosaka, N. Ishii, T. Aida, *Proc. Natl. Acad. Sci. U.S.A.* **2005**, *102*, 10801. e) M. A. Mateos-Timoneda, M. Crego-Calama, D. N. Reinhoudt, *Chem.—Eur. J.* **2006**, *12*, 2630. f) A. Lohr, F. Würthner, *Angew. Chem., Int. Ed.* **2008**, *47*, 1232. g) T. Yamamoto, T. Fukushima, A. Kosaka, W. Jin, Y. Yamamoto, N. Ishii, T. Aida, *Angew. Chem., Int. Ed.* **2008**, *47*, 1672. h) A. Lohr, F. Würthner, *Chem. Commun.* **2008**, 2227.

25 A. Ajayaghosh, R. Varghese, S. J. George, C. Vijayakumar, *Angew. Chem., Int. Ed.* **2006**, *45*, 1141.

26 A. Ajayaghosh, C. Vijayakumar, R. Varghese, S. J. George, *Angew. Chem., Int. Ed.* **2006**, *45*, 456.

27 For cholesterol based self-assembling systems, see: a) S. Shinkai, K. Murata, *J. Mater. Chem.* **1998**, *8*, 485. b) V. A. Mallia, N. Tamaoki, *Chem. Soc. Rev.* **2004**, *33*, 76. c) M. George, R. G. Weiss, *Acc. Chem. Res.* **2006**, *39*, 489.

28 A. Lohr, M. Lysetska, F. Würthner, *Angew. Chem., Int. Ed.* **2005**, *44*, 5071.

29 a) J. S. Moore, *Acc. Chem. Res.* **1997**, *30*, 402. b) D. J. Hill, M. J. Mio, R. B. Prince, T. S. Hughes, J. S. Moore, *Chem. Rev.* **2001**, *101*, 3893. c) M. T. Stone, J. M. Heemstra, J. S. Moore, *Acc. Chem. Res.* **2006**, *39*, 11.

30 a) P. Samorí, V. Francke, K. Müllen, J. P. Rabe, *Chem.—Eur. J.* **1999**, *5*, 2312. b) S. Zahn, T. M. Swager, *Angew. Chem., Int. Ed.* **2002**, *41*, 4225. c) Q. Chu, Y. Pang, *Macromolecules* **2003**, *36*, 4614. d) M. Inouye, M. Waki, H. Abe, *J. Am. Chem. Soc.* **2004**, *126*, 2022. e) R. B. Breitenkamp, G. N. Tew, *Macromolecules* **2004**, *37*, 1163. f) J. Xu, C.-Z. Zhou, L. H. Yang, N. T. S. Chung, Z.-K. Chen, *Langmuir* **2004**, *20*, 950. g) A. Khan, C. Kaiser, S. Hecht, *Angew. Chem., Int. Ed.* **2006**, *45*, 1878.

31 a) A. Ajayaghosh, R. Varghese, V. K. Praveen, S. Mahesh, *Angew. Chem., Int. Ed.* **2006**, *45*, 3261. b) A. Ajayaghosh, R. Varghese, S. Mahesh, V. K. Praveen, *Angew. Chem., Int. Ed.* **2006**, *45*, 7729. c) S. Yagai, S. Mahesh, Y. Kikkawa, K. Unoike, T. Karatsu, A. Kitamura, A. Ajayaghosh, *Angew. Chem., Int. Ed.* **2008**, *47*, 4691.

Ayyappanpillai Ajayaghosh is a native of Kerala, the south west coastal state of India. After his Ph.D. in Chemistry from Calicut University (1988, from the group of Prof. V. N. R. Pillai), he joined the Regional Research Laboratory (presently NIIST) as a scientist. Subsequently he was an Alexander von Humboldt fellow at the Max-Planck-Institut für Strahlenchemie, Müllhein an der Ruhr, Germany (1994–1996) and a visiting scientist to many universities in Germany, Japan and The Netherlands. Currently, he is a Senior Scientist of the National Institute for Interdisciplinary Science and Technology, Trivandrum and an Adjunct Professor of the Material Science Programme of the Indian Institute of Technology, Kanpur. He is a Fellow of the Indian Academy of Sciences and a member of the International Advisory Board, Chemistry: An Asian Journal. His research interests are in the area of photonically and electronically active organic and macromolecular materials, particularly the supramolecular chemistry of functional dyes and π-conjugated systems, molecular self-assemblies, organogels, light harvesting assemblies, and molecular probes.

Vakayil K. Praveen obtained his M.Sc. degree in Applied Chemistry (2001) from Calicut University, Kerala. He completed his Ph.D. from University of Kerala (2007) under the guidance of Dr. A. Ajayaghosh. His Ph.D. work was focused on chromophore based organogels and their application as excitation energy donor scaffolds. Currently he is a Global Centers of Excellence (GCOE) postdoctoral fellow at The University of Tokyo, Japan in the group of Prof. Takuzo Aida.

Sukumaran S. Babu obtained his M.Sc. degree in Polymer Chemistry (2003) from Mahatma Gandhi University, Kerala. Currently he is working as a senior research fellow under the guidance of Dr. A. Ajayaghosh. His research is focused on self-assembly, optical properties, and morphology of linear π-systems.

Chakkooth Vijayakumar obtained his M.Sc. degree in Chemistry from Calicut University, Kerala (2002). He completed his Ph.D. from University of Kerala (2007) under the guidance of Dr. A. Ajayaghosh. His Ph.D. thesis was focused on chromophore self-assemblies and their application as donor scaffolds for resonance energy transfer. Currently he is a postdoctoral fellow at the National Institute for Materials Science (NIMS), Tsukuba, Japan, working in the group of Dr. Masayuki Takeuchi.

Reji Varghese obtained his M.Sc. Degree in Chemistry (2001) from Mahatma Gandhi University, Kottayam, India. He completed his Ph.D. from University of Kerala (2007) on the self-assembly of linearly π-conjugated molecules under the supervision of Dr. A. Ajayaghosh. Currently he is working as an Alexander von Humboldt (AvH) postdoctoral fellow in the group of Prof. H.-A. Wagenknecht at the University of Regensburg on DNA photonics and fluorescent DNA labels.